1-*O*-Alkyl-2-(ω-oxo)acyl-*sn*-glycerols from Shark Oil and Human Milk Fat Are Potential Precursors of PAF Mimics and GHB

Karsten Hartvigsen[a,b] Amir Ravandi[b], Richard Harkewicz[c], Hiroshi Kamido[d], Klaus Bukhave[a], Gunhild Hølmer[a], and Arnis Kuksis[b,*]

[a]Biocentrum-DTU, Biochemistry and Nutrition, Centre for Advanced Food Studies, Technical University of Denmark, DK-2800 Lyngby, Denmark, [b]Banting and Best Department of Medical Research, University of Toronto, Toronto, ON M5G 1L6, Canada, [c]Department of Chemistry and Biochemistry, University of California, La Jolla, California 92093-0601, and [d]Department of Medicine, Kurume University, Kurume, Fukuoka, Japan

ABSTRACT: This study examines the feasibility that peroxidation and lipolysis of 1-*O*-alkyl-2,3-diacyl-*sn*-glycerols (DAGE) found in shark liver oil and human milk fat constitutes a potential source of dietary precursors of platelet activating factor (PAF) mimics and of gamma-hydroxybutyrate (GHB). Purified DAGE were converted into 1-*O*-alkyl-2-acyl-*sn*-glycerols by pancreatic lipase, without isomerization, and transformed into 1-*O*-alkyl-2-oxoacyl-*sn*-glycerols by mild autooxidation. The various core aldehydes without derivatization, as well as the corresponding dinitrophenylhydrazones, were characterized by chromatographic retention time and diagnostic ions by online electrospray mass spectrometry. Core aldehydes of oxidized shark liver oil yielded 23 molecular species of 1-*O*-alkyl-*sn*-glycerols with short-chain *sn*-2 oxoacyl groups, ranging from 4 to 13 carbons, some unsaturated. Autooxidation of human milk fat yielded 1-*O*-octadecyl-2-(9-oxo)nonanoyl-*sn*-glycerol, as the major core aldehyde. Because diradylglycerols with short fatty chains are absorbed in the intestine and react with cytidine diphosphate-choline in the enterocytes, it is concluded that formation of such PAF mimics as 1-*O*-alkyl-2-(ω-oxo)acyl-*sn*-glycerophosphocholine from unsaturated dietary DAGE is a realistic possibility. Likewise, a C_4 core alcohol produced by aldol-keto reduction of a C_4 core aldehyde constitutes a dietary precursor of the neuromodulator and recreational drug GHB, which has not been previously pointed out.

Paper no. L9953 in *Lipids 41*, 679–693 (July 2006).

Platelet-activating factor (PAF), 1-*O*-alkyl-2-acetyl-*sn*-glycerophosphocholine (GroPCho), is a biologically active phospholipid with diverse physiological and pathological effects in a variety of cells and tissues (1). Gamma-hydroxybutyric acid (GHB) is a simple four-carbon FA with an extraordinary range of physiological and pharmacological effects (2). PAF is known to be enzymatically synthesized by either the remodeling or the *de novo* pathways. PAF mimics, however, are generated by secondary peroxidation of unsaturated 1,2-diacyl-*sn*-GroPCho in cell membranes, which retain a short-chain residue esterified at the *sn*-2 position (3). This short-chain residue may contain either a ω-methyl, ω-aldehyde, ω-alcohol, or ω-carboxyl group for PAF-like activity. Investigations of the biological activities by multiple assays have shown that PAF-like lipids containing an *sn*-1 alkyl ether linkage are more effective than the corresponding *sn*-1 acyl derivatives, and that, in general, the shorter the *sn*-2 chain residue the more active the PAF mimic (4,5). Although it has been suggested (2) that GHB may also arise via lipid peroxidation, the exact mechanism has not been established.

In the present report, we demonstrate the feasibility of metabolic transformation of 1-*O*-alkyl-2,3-diacyl-*sn*-glycerols (DAGE) from shark liver oil and human milk into the corresponding core aldehydes, 1-*O*-alkyl-2-(ω-oxo)acyl-*sn*-glycerols, by mild autooxidation and lipolysis. We have previously shown that short-chain 1,2-diradyl-*sn*-glycerols are absorbed intact in the intestine (6,7) and that exogenous 1,2-diradyl-*sn*-glycerols are incorporated intact into the phosphatidylcholines (PtdCho) (8). We have shown elsewhere (9) that such PAF mimics prepared synthetically induce platelet aggregation and inhibit endothelium-dependent arterial relaxation. We postulate that the C_4 core aldehydes, either as glycerolipids or glycerophospholipids, are reduced to the corresponding C_4 core alcohols by endogenous aldol-keto reductases (10) before release into circulation as GHB. There has been no previous work on the core aldehydes arising from oxidation of alkyldiacylglycerols, although the nonvolatile oxidation products of triacylglycerols have been previously discussed (11–16).

EXPERIMENTAL PROCEDURES

Materials. Crude deep-sea shark liver oil was a gift from Baldur Hjaltason, LYSI Ltd., Reykjavik, Iceland. The lyophilized

*To whom correspondence should be addressed at Banting and Best Department of Medical Research, University of Toronto, 112 College Street, Toronto, ON M5G 1L6, Canada. E-mail: arnis.kuksis@utoronto.ca

Present address of first author: Department of Medicine, University of California, La Jolla, CA 92093-0682. Present address of fourth author: Midori Health Care Foundation, 3-22-5 Tarumi-cho, Suita, Osaka 564-0062, Japan. Present address of fifth author: Department of Human Nutrition, The Royal Veterinary and Agricultural University, DK-1958, Frederiksberg, Denmark.

Abbreviations: CapEx, capillary exit; CDP, cytidine diphosphate; DAGE, 1-*O*-alkyl-2,3-diacyl-*sn*-glycerol; DNPH, 2,4-dinitrophenylhydrazine; GE, 1-*O*-alkyl-*sn*-glycerol; GHB, gamma-hydroxybutyric acid; GroPCho, glycerophosphocholine; LC/ESI-MS, LC/electrospray ionization/MS; 2-MAGE, 1-*O*-alkyl-2-acyl-*sn*-glycerol; 3-MAGE, 1-*O*-alkyl-3-acyl-*sn*-glycerol; PAF, platelet-activating factor; PtdCho, phosphatidylcholines (PtdCho); R_f, relative retention factor; RT, retention time.

human milk sample was a gift from Dr. J. Cerbulis of the Eastern Regional Research Center, USDA, Philadelphia, PA. It was one of six milk samples obtained from nursing mothers in the Philadelphia area and used in a collaborative investigation of chloropropanediol diesters in human milk samples (17). The alkyldiacylglycerol composition of these samples ranged from 0.5 to 5 mol%. Linoleic acid, 4-dimethylaminopyridine, and *N*,*N*′-dicyclohexylcarbodiimide were obtained from Sigma-Aldrich (St. Louis, MO). 1-*O*-Octadecyl-*sn*-glycerol was obtained from Fluka (Ronkonkoma, NY). All solvents used were of analytical or HPLC grade.

Preparative TLC. Several preparative TLC systems were employed to purify the various transformation products. All TLC plates were prepared in the laboratory (200 × 200 × 0.25 mm) and activated for 2 h at 110°C before use. System A consisted of silica gel H, developed in hexane/diethyl ether (90:10, vol/vol). System B consisted of silica gel G containing 5% boric acid, developed in hexane/isopropyl ether/acetic acid (50:50:4, by vol). System C consisted of silica gel H, developed in hexane/diethyl ether/acetic acid (80:20:2, by vol). Lipids were visualized under UV light after spraying with 0.2% 2,7-dichlorofluorescein in ethanol (18), whereas the core aldehydes were visualized as purple areas after spraying with the Schiff base reagent (19). Migration of a component is given as the relative retention factor (R_f). Lipids and core aldehydes were recovered from the TLC plates by scraping off the gel, extracting it with chloroform/methanol (2:1, vol/vol), washing with water, drying over anhydrous sodium sulfate, evaporating under nitrogen, and dissolving in chloroform/methanol (2:1, vol/vol). The 2,7-dichlorofluorescein was removed with 1% ammonium hydroxide.

GLC. Injections were made at 100°C, and after 30 s the oven temperature was programmed at 20°C/min to either 130°C (FAME) or 180°C (diacetyl-derivatized 1-*O*-alkyl-*sn*-glycerols (GE)), and then to 240°C at 5°C/min (18). The GLC system consisted of a polar capillary column (SP 2380, 15 m × 0.32 mm i.d., Supelco, Mississauga, ON) installed in a Hewlett-Packard (Palo Alto, CA) Model 5880 gas chromatograph equipped with a flame ionization detector. Hydrogen was used as carrier gas at 3 psi. FAME and diacetyl-GE were identified on the basis of retention times (RT) compared with commercially available external reference compounds.

HPLC. Reversed-phase HPLC was performed with a Hewlett-Packard Model 1090 liquid chromatograph (Palo Alto, CA) using an HP ODS Hypersil C_{18} column (5 μm; 200 × 2.1 mm i.d.; Hewlett-Packard, Palo Alto, CA) and eluted isocratically with 100% Solvent A (methanol/water/30% ammonium hydroxide, 88:12:0.5, by vol) for 3 min, followed by a linear gradient to 100% Solvent B (methanol/hexane/30% ammonium hydroxide, 88:12:0.5, by vol) in 25 min, which was kept for another 6 min (20). Kim *et al.* (20) washed the HPLC column with 0.1 M ammonium acetate at 0.5 mL/min for 5 min at the end of each run and did not observe any ill effects on the performance of column or the quality of the mass spectra. When 2,4-dinitrophenylhydrazine (DNPH) derivatives were analyzed, the effluent was led through a UV detector (358 nm) installed before the mass spectrometer. The flow was 0.4 mL/min.

Electrospray ionization MS (ESI-MS). Reversed-phase HPLC with online electrospray ionization MS (LC/ESI-MS) was performed by admitting the entire HPLC column effluent into a Hewlett-Packard Model 5988B quadrupole mass spectrometer (Palo Alto, CA) equipped with a nebulizer-assisted electrospray interface (Hewlett-Packard Model 59987A, Palo Alto, CA) as previously described (19). Nitrogen was used as both nebulizing (60 psi) and drying gas (60 psi, 270°C). Capillary voltage was set at 4 kV, the endplate voltage was 3.5 kV, and the cylinder voltage was 5 kV in the positive mode of ionization. In the negative mode, the values were −3.5 kV, −3 kV, and −3.5 kV, respectively. Both negative and positive ESI spectra were taken in the mass range 300–1100 amu. The capillary exit (CapEx) was set at 120 and −120 V in the positive and negative ion mode, respectively.

Preparation of DAGE from shark liver oil and human milk. A total lipid extract of freeze-dried human milk was prepared as previously described (21). DAGE was recovered from the human milk lipid extract and the shark liver oil by preparative double one-dimensional TLC (system A). The purified DAGE was subjected to regiospecific analysis to reveal the *sn*-1-*O*-alkyl-, *sn*-2 acyl-, and *sn*-3 acyl-chain composition and distribution. The complete procedure is outlined in Scheme 1.

Hydrolysis with pancreatic lipase and Grignard degradation. Purified DAGE of shark liver oil and human milk were hydrolyzed by digestion with diethyl ether pre-extracted pancreatic lipase (22). The digestion was performed in the presence of gum arabic for 30 min, and the digestion products were extracted with diethyl ether. Alternatively, the purified DAGE were deacylated by Grignard degradation (23) in order to verify the results obtained from pancreatic lipase digestion. The degradation products were resolved and recovered by TLC (system B).

Preparation of FAME and diacetyl-GE. Purified fractions of DAGE, 2-MAGE, and 3-MAGE originating from shark liver oil were treated with 6% H_2SO_4 in methanol for 2 h at 80°C to produce FAME and GE. After the reaction, the lipids were extracted twice with chloroform. GE and FAME were resolved and recovered by preparative TLC (system C). Purified GE was derivatized to diacetyl-GE for 30 min at 80°C with acetic anhydride/pyridine (1:1, vol/vol; 75 μL). The profiles of FAME and diacetyl-GE were determined by GLC.

Autooxidation of 2-MAGE. Mild peroxidation was performed by flushing the purified 2-MAGE from either shark liver oil or human milk in a tube with oxygen, capping, and heating at 80°C for 3 h. The peroxidized 2-MAGE was analyzed by reversed-phase LC/ESI-MS.

Preparation of DNPH derivatives. Aldehyde preparations of oxidized 2-MAGE were derivatized by reaction with DNPH in the dark (0.5 mg in 1 mL 1 N HCl) for 2 h at room temperature and 1 h at 4°C (24). The DNPH derivatives were extracted with chloroform/methanol (2:1, vol/vol), dried over anhydrous sodium sulfate, evaporated under a stream of nitrogen, dissolved in chloroform/methanol (2:1, vol/vol), and analyzed by

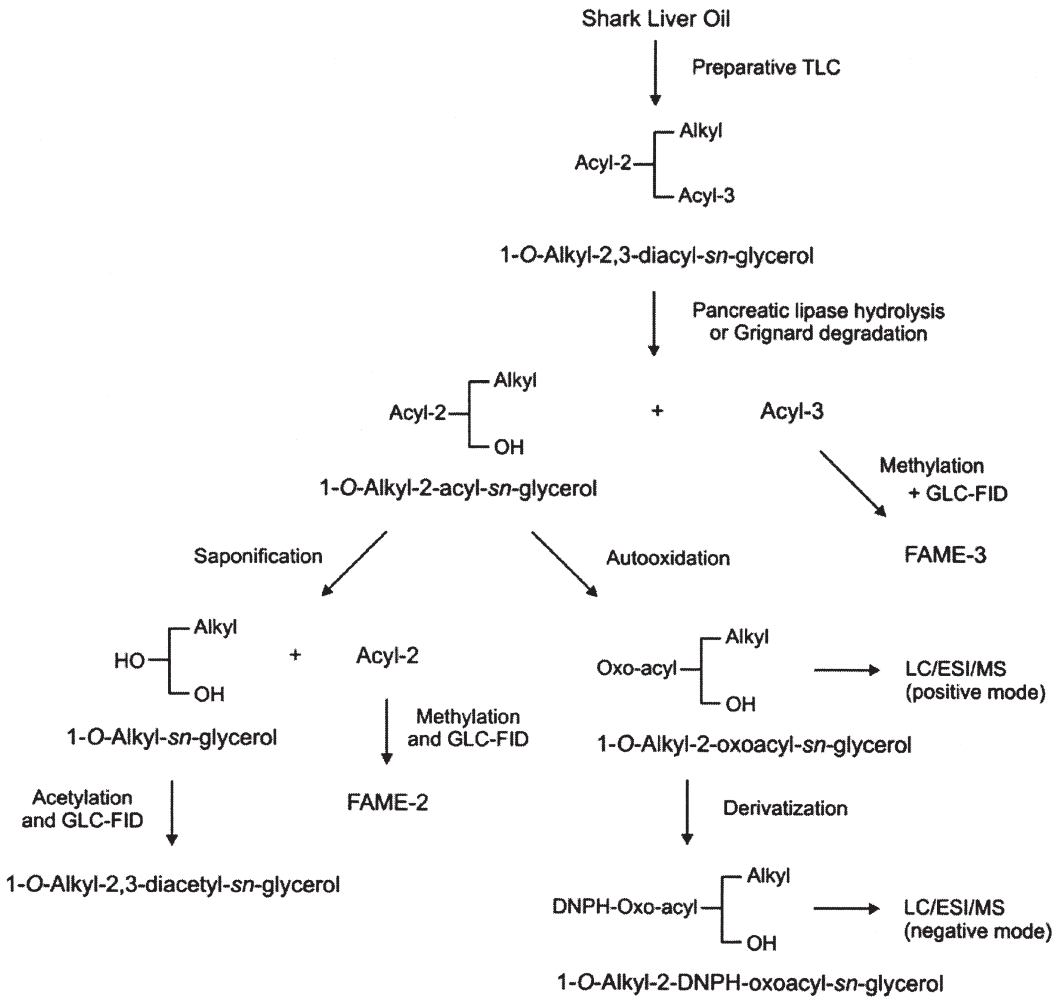

SCHEME 1. Flow sheet for the regiospecific analysis of DAGE from shark liver oil and the procedure for isolation and characterization of core aldehydes from oxidized and digested DAGE.

reversed-phase LC/ESI-MS. Derivatization with DNPH, therefore, increased the detection limit for the core aldehydes by MS, and further provided additional ions for characterization of the alkyl ether core aldehydes, as well as an opportunity to monitor the components by UV detection at 358 nm.

Preparation of reference 1-O-octadecyl-2-(9-oxo)-nonanoyl-sn-glycerol. The esterfication of 1-*O*-octadecyl-*sn*-glycerol with linoleic acid was performed by the carbodiimide-mediated process (25). Linoleic acid (75 μmol), 1-*O*-octadecyl-*sn*-glycerol (100 μmol), and 4-dimethyl-aminopyridine (10 μmol) were dissolved in dry n-hexane. This solution was added to a suspension of *N*,*N*′-dicyclohexylcarbodiimide (100 μmol) in dry n-hexane and shaken vigorously for 17 h at room temperature. After filtration, solvent was evaporated under nitrogen, and the residue was purified by preparative TLC (system B). We have previously reported the LC/ESI-MS analysis of this and other related synthetic neutral ether lipids (26).

The synthesized and purified 1-*O*-octadecyl-2-octadecadienoyl-*sn*-glycerol was subjected to triphenylphosphine reductive ozonization as previously described (19). The resulting reference core aldehyde, 1-*O*-octadecyl-2-(9-oxo)nonanoyl-*sn*-glycerol (R_f = 0.11), was purified by preparative TLC (system B) and analyzed by reversed-phase LC/ESI-MS, and its identity was established on basis of RT, averaged mass spectrum, and fragmentation pattern.

RESULTS

Isolation of DAGE. Preparative TLC resolved the crude shark liver oil into six bands, which corresponded to monoacyl (monoradyl) glycerols (R_f = 0.01), free cholesterol (R_f = 0.13), triacylglycerol (R_f =0.37), DAGE (R_f = 0.55), cholesteryl esters (R_f = 0.93), and squalene (R_f = 0.97). The TLC bands were scraped off the plate and analyzed by high-temperature GLC, which indicated that the DAGE made up 55% of the shark liver oil. Reversed-phase LC/ESI-MS indicated that DAGE was composed of at least 50 species eluting between 10 and 37 min (chromatogram not shown). Similarly, the DAGE content of human milk was estimated to be approximately 1% of total fat and was made up of numerous species, of which only a few were abundant.

Regiospecific analysis of DAGE (26). The purified DAGE were subjected to a regiospecific analysis to reveal the *sn*-1-*O*-

alkyl, *sn*-2-acyl, and *sn*-3-acyl chain composition and distribution, which were determined by TLC (system B) and GLC, following pancreatic lipase hydrolysis and Grignard degradation.

Pancreatic lipase hydrolysis of the DAGE yielded 1-*O*-alkyl-2-acyl-*sn*-glycerols (2-MAGE, R_f = 0.32) as the major product (97%) and 1-*O*-alkyl-3-acyl-*sn*-glycerol (3-MAGE, R_f = 0.41) as the minor product (3%), along with GE (R_f = 0.05), free FA (R_f = 0.66), and original DAGE (R_f = 0.90).

The high recovery of 2-MAGE compared with 3-MAGE is consistent with the resistance of the *sn*-1 ether linkage to the action of most enzymes, and furthermore indicates a very low rate of isomerization and a low affinity of the pancreatic lipase for the *sn*-2-position of DAGE. The non-selective Grignard degradation yielded the 2-MAGE and 3-MAGE in equal amounts together with GE and the free FA as the tertiary alcohols (Grignard reaction products). The DAGE, 2-MAGE, and 3-MAGE fractions recovered from the pancreatic lipase digestion and Grignard degradation were treated with sulfuric acid/methanol to produce FAME and glyceryl ethers (GE), which were resolved by preparative TLC (system C). The purified GE were converted into the diacetyl GE by reaction with acetic anhydride and pyridine, and the FAME and the GE acetates were identified and quantified by GLC. Reversed-phase LC/ESI-MS analysis of 2-MAGE isolated from the shark liver oil following pancreatic lipolysis of DAGE showed a total of 49 species, of which 20 species were abundant, eluting between 10 and 26 min (chromatogram not shown).

Table 1 gives the regiospecific distribution of the fatty chains of shark liver oil DAGE as determined by GLC analysis of products of pancreatic lipolysis and Grignard degradation. The predominant *sn*-1-*O*-alkyl fatty chains were the monounsaturated alcohols (18:1n-9, 54.9%, and 16:1n-7, 12.2%) and saturated alcohols (16:0, 11.2%), with much smaller amounts of a diunsaturated alcohol (18:2n-6, 1%). Small amounts of odd-carbon saturated and monounsaturated fatty alcohols were also detected. Pancreatic lipase digestion and Grignard degradation gave similar FA profiles and selectivity for the *sn*-2- and *sn*-3-positions. The most abundant *sn*-2-FA were 16:0, 16:1n-7, 18:1n-9, 20:1n-9, 22:1n-11/13, 22:5n-3, and 22:6n-3, with 18:1n-9 accounting for more than 50% of the total. The most abundant *sn*-3-FA were 16:0, 16:1n-7, 18:0, 18:1n-9, 20:1n-9, 22:1n-11/13, and 22:4n-3. The FA 18:1n-9, 22:5n-3, and 22:6n-3 were preferentially associated with the *sn*-2-position, whereas 18:0, 20:1n-9, 22:1n-11/13, and 22:4n-3 were mostly in the *sn*-3-position.

LC/ESI-MS characterization of reference core aldehydes. The identities of all synthetic neutral ether lipids were established by combined TLC and LC/ESI-MS analysis. The 1-*O*-octadecyl-2-(9-oxo)nonanoyl-*sn*-glycerol was produced in high yield and purity by reductive ozonization of 1-*O*-octadecyl-2-(9-*cis*,12-*cis*)-octadecadienoyl-*sn*-glycerol. Figure 1A shows the total LC/ESI-MS positive ion current profile (CapEx +120 V) of synthetic 1-*O*-octadecyl-2-(9-oxo)nonanoyl-*sn*-glycerol (RT = 14.8 min). Figure 1B shows the full mass spectrum averaged over the entire peak with eight major ions being observed. The assignments for the observed ions, their corre-

TABLE 1
Regiospecific Distribution (mol%) of FA of Shark Liver Oil DAGE as Determined by GLC-FID After Pancreatic Lipase Hydrolysis or Grignard Degradation[a]

		sn-2 Acyl		*sn*-3 Acyl	
Fatty chain	*sn*-1 Alkyl	Lipase	Grignard	Lipase	Grignard
12:0	1.0	nd	nd	nd	nd
14:0	2.3	1.0	1.4	0.7	0.8
15:0	0.4	0.3	0.3	0.1	0.2
16:0	11.2	18.4	18.8	15.9	19.5
16:1n-7	12.2	4.7	4.9	3.2	3.2
16:2n-4	nd	0.7	0.7	0.9	1.0
17:0	0.6	nd	nd	nd	nd
17:1	2.2	nd	nd	nd	nd
18:0	2.9	1.2	1.7	4.6	3.7
18:1n-9	54.9	51.8	48.9	21.3	16.9
18:1n-7	4.6	nd	0.3	5.8	6.6
18:2n-6	1.0	0.8	0.8	0.7	0.2
18:3n-3	nd	0.3	0.4	0.4	0.3
18:4n-3	nd	0.2	0.2	0.2	0.1
19:0	0.6	nd	nd	nd	nd
20:1n-9	2.6	6.1	5.5	11.1	12.4
20:2n-6	nd	0.1	0.2	0.3	0.3
20:4n-6	nd	nd	0.1	nd	nd
20:5n-3	nd	0.1	0.3	0.5	0.2
22:1n-11/13	0.2	3.7	3.4	18.0	21.0
22:4n-3	nd	0.2	0.2	5.9	7.4
22:5n-3	nd	1.6	1.4	0.5	0.4
22:6n-3	nd	4.1	3.3	1.5	0.8
24:1n-3	nd	0.7	0.9	0.3	0.2

[a]Average of two determinations. nd, not detected.

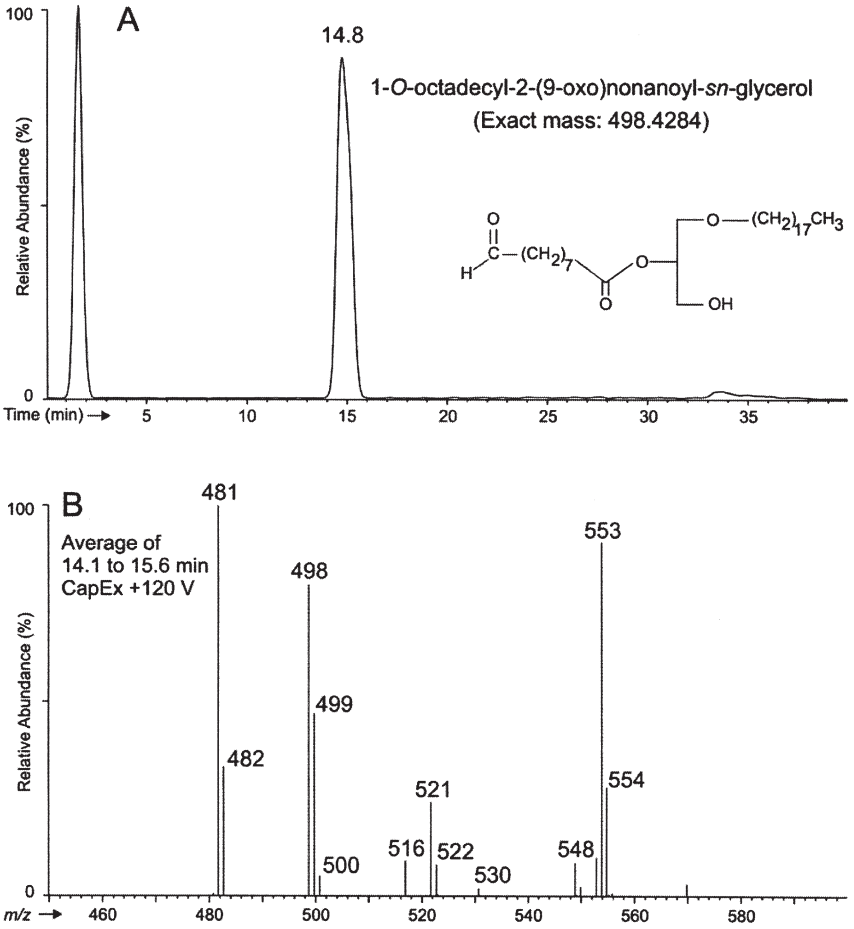

FIG. 1. Reversed-phase LC/ESI-MS analysis of synthetic 1-*O*-octadecyl-2-(9-oxo)nonanoyl-*sn*-glycerol. (A) Total positive ion current profile. (B) Full mass spectrum averaged over the entire peak, zoomed to *m/z* 450–600, in (A). All of the ions detected in the spectrum were assigned to the original reference compound. Note the high abundance for the *m/z* 499 ion relative to *m/z* 498, suggesting that the *m/z* 499 ion is not entirely composed of the ^{13}C isotopic ion of *m/z* 498. The LC/ESI-MS analysis showed that the optimal diagnostic ion of the 1-*O*-alkyl-2-(ω-oxo)acyl-*sn*-glycerols is the $[M - 17]^+$ ion, which in (B) corresponds to *m/z* 481. Additional details are given in Table 2, Scheme 2, and the text.

sponding ^{13}C isotopic components, and their relative abundances are presented in Table 2. The proposed molecular structures for these assigned ions are shown in Scheme 2. Sodium and ammonium adducts are common features of ESI, and it is also known that aldehydes in methanol solutions, as encountered in the mobile phase, are converted to the corresponding neutral hemi-acetal form (a methanol adduct).

The presence of an ion at *m/z* 498.70 corresponding to the $[M]^+$ ion was unexpected and only observed in the samples with the underivatized monoalkylglycerols containing a free aldehyde ester group. We confirmed this observation with the corresponding 3-isomer reference compound, 1-*O*-octadecyl-3-(9-oxo)nonanoyl-*sn*-glycerol (data not shown). It would be expected that the observed ion would have *m/z* 499.75 corresponding to the protonated molecular ion $[M + H]^+$. As indicated in Table 2 and Scheme 2, we propose that the $[M]^+$ ion at *m/z* 498.70 arises from a dehydrated ammonium adduct, $[M + NH_4 - H_2O]^+$, and not directly from the ionization as a radical cation, $[M]^{+\cdot}$. Another unexpected observation was the relatively high abundance (59%) of the *m/z* 499.75 ion compared with the *m/z* 498.70 ion, which is much higher than the calculated contribution of the ^{13}C isotope (32%) for this compound. The other ions have the ^{13}C contribution showing the expected ~32% relative abundance (Table 2). This suggests that the peak at *m/z* 499.75 is actually composed of two different species, $[(M + {}^{13}C_1) + NH_4 - H_2O]^+$ and the protonated molecular ion, $[M + H]^+$. As indicated in Table 2 and Scheme 2, we propose that the $[M + H]^+$ ion can also arise indirectly from the neutral loss of ammonia from the molecular ammonium adduct, $[M + NH_4 - NH_3]^+$.

Due to the lengthy and complicated ion assignment and the multiple possible pathways of ion formation, we have decided to describe the ions as mass difference from the exact mass of the 1-*O*-alkyl-2-(ω-oxo)-*sn*-glycerol, that is, $[M \pm X]^+$.

TABLE 2
Mass Spectrometric Analysis of Synthetic 1-*O*-Octadecyl-2-(9-Oxo)Nonanoyl-*sn*-Glycerol: Assignment of Detected Ions Including Corresponding ^{13}C Isotopic Ions and Their Relative Abundance[a]

Ion ID	Ion (m/z) (Rel. Ab.)[b]	^{13}C Ion (m/z)	(Rel. Ab.)	Ion assignment
$[M - 17]^+$	481.65 (100%)	+1	482.65 (33%)	$[M + H - H_2O]^+$ and/or $[M + NH_4 - NH_3 - H_2O]^+$
$[M]^+$	498.70 (80%)	+1	499.75 (32%)[c]	$[M + NH_4 - H2O]+$
$[M + 1]^+$	499.75 (21%)[d]	+1	500.75 (24%)[e]	$[M + H]^+$ and/or $[M + NH_4 - NH_3]^+$
$[M + 18]^+$	516.70 (9%)			$[M + NH_4]^+$
$[M + 23]^+$	521.70 (24%)	+1	522.70 (33%)	$[M + Na]^+$
$[M + 32]^+$	530.70 (2%)			$[M + CH_3OH + NH_4 - H_2O]^+$
$[M + 50]+$	548.70 (9%)	+1	549.80 (31%)	$[M + CH_3OH + NH_4]+$
$[M + 55]^+$	553.85 (91%)	+1	554.75 (31%)	$[M + CH_3OH + Na]+$

[a]Average of four mass spectra.
[b]Rel. Ab., relative ion abundance.
[c]Calculated Rel. Ab. based on expected ^{13}C contribution and the average of the other detected ^{13}C isotopic ions.
[d]Calculated Rel. Ab. as the total ion abundance for *m/z* 499.75 subtracted the contribution from the ^{13}C isotopic ion of *m/z* 498.70; calculated Rel. Ab. based on the calculated ion abundance. Additional details are given in Figure 1, Scheme 2, and the text.
[e]Calculated Rel. Ab. based on the calculated ion abundance for m/z 499.75 [M+1]+, see [d].

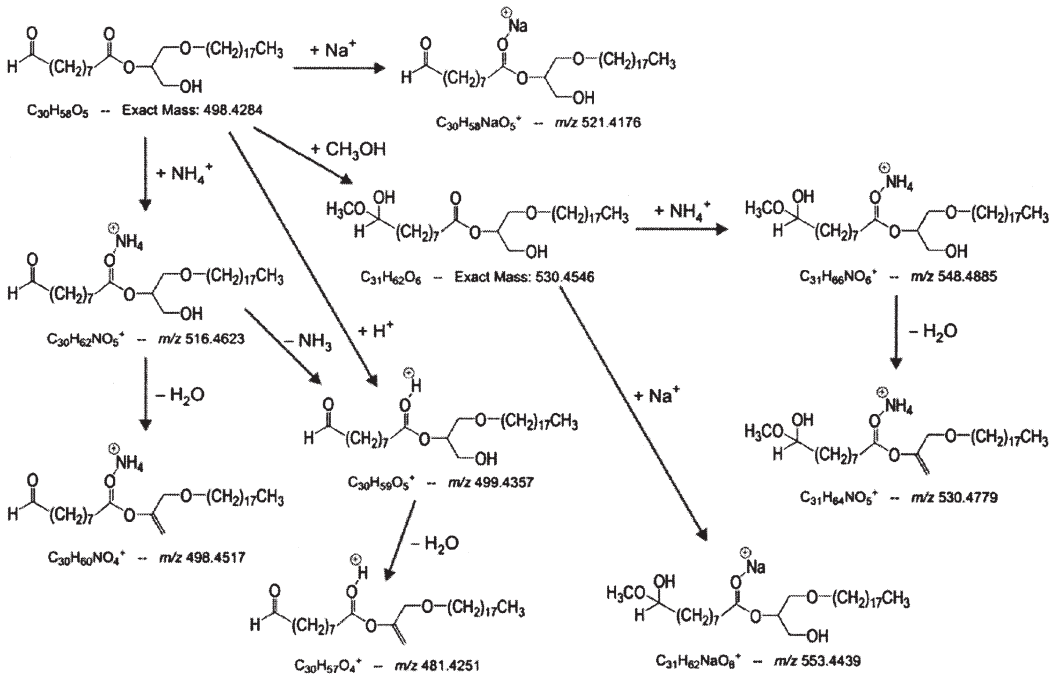

SCHEME 2. Proposed ionization and formation of various ions in the spectrum of synthetic 1-*O*-octadecyl-2-(9-oxo)nonanoyl-*sn*-glycerol. Additional details are given in Figure 1, Table 2, and the text.

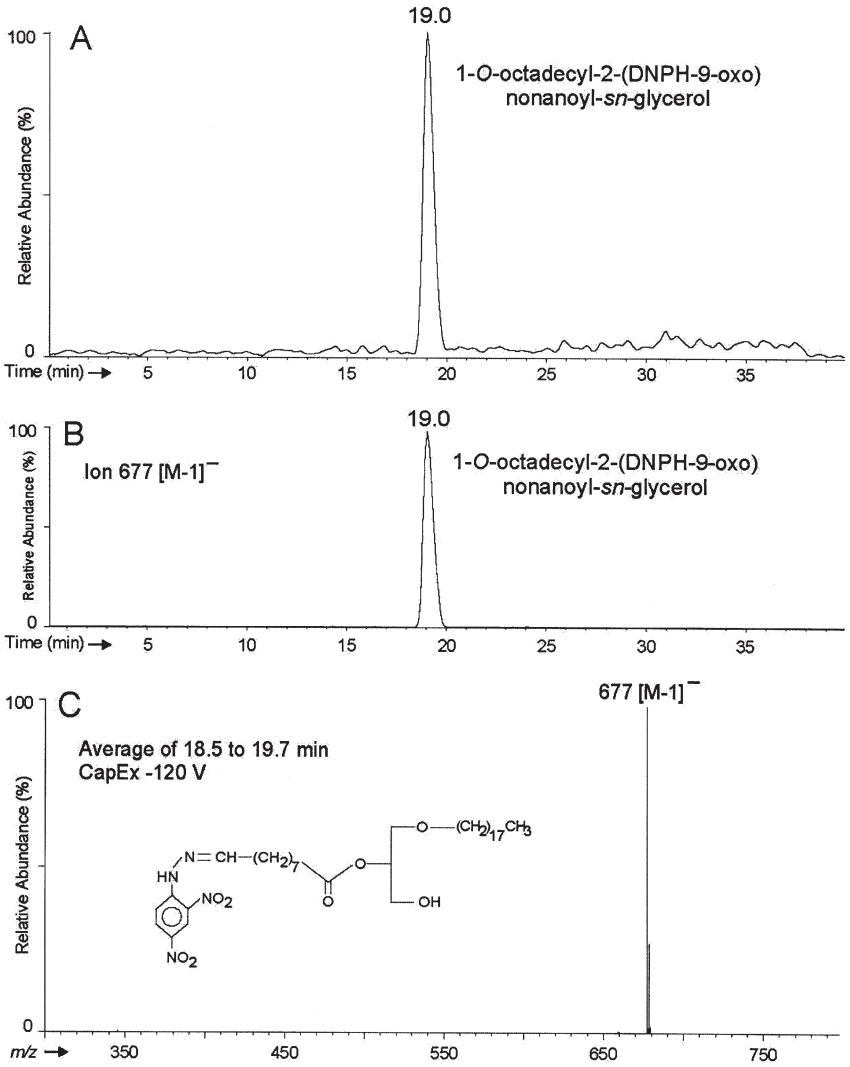

FIG. 2. Reversed-phase LC/ESI-MS analysis of synthetic and DNPH derivatized 1-*O*-octadecyl-2-(9-oxo)nonanoyl-*sn*-glycerol. (A) Total negative ion current profile. (B) Reconstructed single-ion chromatogram of the *m/z* 677 $[M - 1]^-$ ion. (C) Full mass spectrum averaged over the entire peak, zoomed to *m/z* 300–800, in (A). The diagnostic ion of 1-*O*-alkyl-2-(DNPH-oxo)acyl-*sn*-glycerols is thus the $[M - 1]^-$ ion.

The best diagnostic ion of 1-*O*-alkyl-2-oxoacyl-*sn*-glycerols under our experimental LC/ESI-MS conditions was the $[M - 17]^+$ ion at *m/z* 481.65, which we propose arises from the dehydration of the *m/z* 498.70 $[M + 1]^+$ ion (Fig. 1B, Table 2, and Scheme 2).

Further identification of 1-*O*-octadecyl-2-(9-oxo)nonanoyl-*sn*-glycerol was performed by derivatization with DNPH. Figure 2 shows the total LC/ESI-MS negative ion current profile with CapEx at −120 V of the DNPH-derivatized 1-*O*-octadecyl-2-(9-oxo)nonanoyl-*sn*-glycerol (RT 19.0 min, Fig. 2A) along with the reconstructed single-ion chromatogram (Fig. 2B) for the $[M - 1]^-$ ion, and the full mass spectrum (Fig. 2C) averaged over the entire peak. As demonstrated in Figure 2C, 1-*O*-octadecyl-2-(DNPH-9-oxo)nonanoyl-*sn*-glycerol was characterized by the deprotonated molecular ion, $[M - 1]^-$ at *m/z* 677, which was used as the diagnostic ion.

Characterization of 2-MAGE core aldehydes in autooxidized shark liver oil. Figure 3 shows the total positive ion current profile of the 1-*O*-alkyl-2-acyl-*sn*-glycerols before autooxidation (Fig. 3A) and after 3 h autooxidation (Fig. 3B) of shark liver oil 2-MAGE. The resulting ether core aldehydes (i.e., 1-*O*-alkyl-2-(ω-oxo)acyl-*sn*-glycerols) eluted with retention times ranging from 9 to 15 min, the hydroperoxides (i.e., 1-*O*-alkyl-2-(hydroperoxy)acyl-*sn*-glycerols) and other oxidation products with retention times ranging from 5 to 25 min, and the non-oxidized 1-*O*-alkyl-2-acyl-*sn*-glycerols with retention times from 25 to 35 min. The core aldehydes made up about 5%, and the other oxidation products about 40%, of the total peak area (Fig. 3B). Figure 3 also shows the reconstructed single-ion chromatograms for the $[M - 17]^+$ ion of 1-*O*-octadecenyl-2-(4-oxo)butyroyl-*sn*-glycerol (Fig. 3C) and 1-*O*-octadecenyl-2-(9-oxo)nonanoyl-*sn*-glycerol (Fig. 3D). Several 1-*O*-

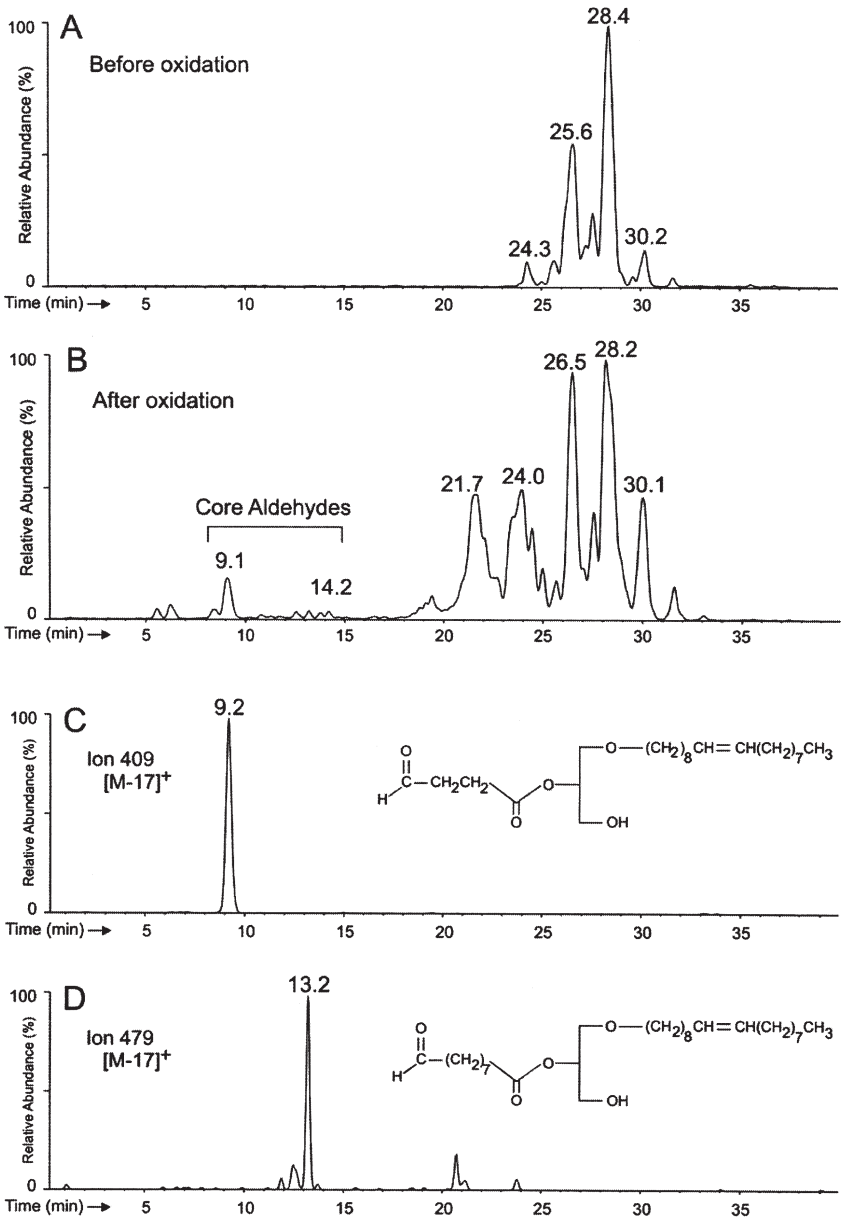

FIG. 3. Reversed-phase LC/ESI-MS analysis of 1-*O*-alkyl-2-acyl-*sn*-glycerols isolated from shark liver oil before and following oxidation. (A) and (B) Total positive ion current profiles of non-oxidized and autooxidized (80°C for 3 h in oxygen atmosphere) 1-*O*-alkyl-2-acyl-*sn*-glycerols, respectively. (C) and (D) reconstructed single-ion chromatograms of the *m/z* 409 and 479 $[M - 17]^+$ diagnostic ion of 1-*O*-octadecenyl-2-(4-oxo)butyroyl-*sn*-glycerol and 1-*O*-octadecenyl-2-(9-oxo)nonanoyl-*sn*-glycerol, respectively.

alkyl-2-oxoacyl-*sn*-glycerols were identified on the basis of the $[M - 17]^+$ and $[M]^+$ ions (Table 3). The major ether core aldehydes corresponded to 18:1-4:0Ald (20%), 16:1-9:0Ald (18:1-7:0Ald) (10%), 16:0-9:0Ald (2%), 16:0-10:1 (17:1-9:0Ald) (2%), 18:1-9:0Ald (20%), and 18:1-10:1Ald (7%).

Figure 4 shows the total LC/ESI-MS negative ion current profile (Fig. 4A) of DNPH-derivatized and purified 1-*O*-alkyl-2-oxoacyl-*sn*-glycerol, derived from shark liver oil DAGE, along with selected, reconstructed single-ion mass chromatograms for the $[M - 1]^-$ ion of 1-*O*-hexadecenyl-2-(DNPH-4-oxo)butyroyl-*sn*-glycerol (Fig. 4B), 1-*O*-hexadecyl-2-(DNPH-4-oxo)butyroyl-*sn*-glycerol (Fig. 4C), 1-*O*-octadecenyl-2-(DNPH-4-oxo)butyroyl-*sn*-glycerol (Fig. 4D), 1-*O*-octadecenyl-2-(DNPH-7-oxo)heptanoyl-*sn*-glycerol (Fig. 4E), 1-*O*-octadecenyl-2-(DNPH-9-oxo)nonanoyl-*sn*-glycerol (Fig. 4F), and 1-*O*-octadecyl-2-(DNPH-9-oxo)nonanoyl-*sn*-glycerol (Fig. 4G), which all were eluted over the time period of 10 to 20 min.

Table 4 lists the identified molecular species along with the uncorrected peak areas attributed to them. The $[M - 1]^-$ ion provides only the molecular weight of the compound. Further

TABLE 3
Identification of Molecular Species of 1-*O*-Alkyl-2-Oxoacyl-*sn*-Glycerols, Produced by Autooxidation of Pancreatic Lipase Treated Shark Liver Oil DAGE and Estimated by LC/ESI-MS[a]

Molecular species		1-*O*-Alkyl-2-oxoacyl-*sn*-glycerol		
Carbon number	Tentative identity	RT (min)	$[M]^+$ (m/z)	$[M - 17]^+$ (m/z)
22:1 Ald	18:1-4:0 Ald	9.2	426	409
25:1 Ald	16:1-9:0 Ald 18:1-7:0 Ald	11.0	nd	451
25:0 Ald	16:0-9:0 Ald	11.3	nd	453
26:1 Ald	16:0-10:1 Ald 17:1-9:0 Ald	11.7	nd	465
27:1 Ald	18:1-9:0 Ald	12.6	496	479
28:2 Ald	18:1-10:1 Ald	13.2	508	491

[a]Two analyses. RT, retention time; Ald, aldehyde; nd, not detected.

confirmation of the structure was obtained from the linear correlation ($R = 0.982$) obtained between retention time and molecular mass among the 1-*O*-alkyl-2-DNPH-oxoacyl-*sn*-glycerols, when the latter was calculated as the total carbon number minus one carbon per double bond (Table 4). This elution factor makes it possible to calculate the relative retention times of unknowns with considerable accuracy, which helped to choose among likely structures represented by the same molecular mass within the reversed-phase LC/ESI-MS profile. Further characterization of the molecular species was obtained from knowledge of the possible formation of esterified aldehyde residues and the ratios of the corresponding *sn*-1 and *sn*-2 fatty chain moieties (Tables 1 and 4). For example, the masses at *m/z* 577 and 579 ($[M - 1]^-$ ions) can only represent the 1-*O*-hexadecenyl- and 1-*O*-hexadecyl-2-(DNPH-4-oxo)butyroyl-*sn*-glycerols (Figs. 4B and 4C), respectively. The ion at *m/z* 605 $[M - 1]^-$, however, could represent both the 1-*O*-octadecenyl-2-(DNPH-4-oxo)butyroyl-*sn*-glycerol and the 1-*O*-pentadecyl-2-(DNPH-7-oxo)heptanoyl-*sn*-glycerols (Table 4 and Fig. 4D), but on the basis of the much higher abundance of *sn*-1 alkyl 18:1n-9 in comparison with 15:0 (Table 1), it is obvious that the peak area mainly represents the 1-*O*-octadecenyl-2-(DNPH-4-oxo)butyroyl-*sn*-glycerol. The alternative identities of the species are written in parentheses in Table 4.

Characterization of 2-MAGE core aldehydes in autooxidized human milk. The small DAGE fraction isolated from human milk fat yielded a 1-*O*-hexadecylglycerol and oleic acid from the *sn*-2- and *sn*-3-positions as the major fatty chains. Figure 5 shows the total LC/ESI-MS negative ion current profile (Fig. 5A) of DNPH-derivatized 1-*O*-alkyl-2-oxoacyl-*sn*-glycerols, derived from human milk DAGE, along with the reconstructed single-ion mass chromatogram (Fig. 5B) for the $[M - 1]^-$ ion of 1-*O*-octadecyl-2-(DNPH-9-oxo)nonanoyl-*sn*-glycerol (RT = 18.8 min), and the full mass spectrum (Fig. 5C) averaged over the entire peak. This was the only ether core aldehyde characterized from human milk.

DISCUSSION

The major source of PAF-like lipids (or mimics/analogues) is the unregulated oxidative modification of cellular and plasma phospholipids. There have been numerous reports on isolation of the PAF-like lipids containing a long-chain fatty ester in the *sn*-1-position and a short-chain (ω-oxo)acyl group in the *sn*-2-position of PtdCho (27). The immediate precursors of these mimics are the 1,2-diacyl- and 1-*O*-alkyl-2-acyl-*sn*-GroPCho with saturated acyl and alkyl chains in the *sn*-1-position. Among these, the most frequently reported are 1-hexadecanoyl- and 1-octadecanoyl-2-(5-oxo)pentanoyl-*sn*-GroPCho, which are generated from the corresponding arachidonates (27). The corresponding *sn*-1 alkyl ether derivative, which is structurally more closely related to PAF, has been studied less frequently due to the more limited supply of potential precursors, although it was the first PAF analogue identified (27) and both DAGE and 1-*O*-alkyl-2-acyl-*sn*-glycerophospholipids are present in significant amounts of tissue lipids (28). The present study demonstrates the feasibility of generating PAF analogue precursors in the intestine by lipolysis and peroxidation of the DAGE, which constitute a significant proportion of dietary fats such as shark liver oil and milk fat. In addition, this study has recognized certain unusual features of 1-*O*-alkyl-2-(ω-oxo)acyl-*sn*-glycerols as precursors of PAF analogues. The 1,2-diradyl-*sn*-glycerol moieties generated from DAGE of shark liver oil were characterized by the presence of sites of unsaturation in both fatty chains. The peroxidation would, therefore, be expected largely to affect the 18:2n-6, 18:3n-3, and especially the 22:5n-3 and 22:6n-3, which would be anticipated to yield C_4 to C_9 core aldehydes in combination with both saturated and monounsaturated alkyl chains in the *sn*-1-position. The present results confirm that peroxidation of the monounsaturated 1-*O*-alkyl chains was limited during the mild conditions as previously described (29).

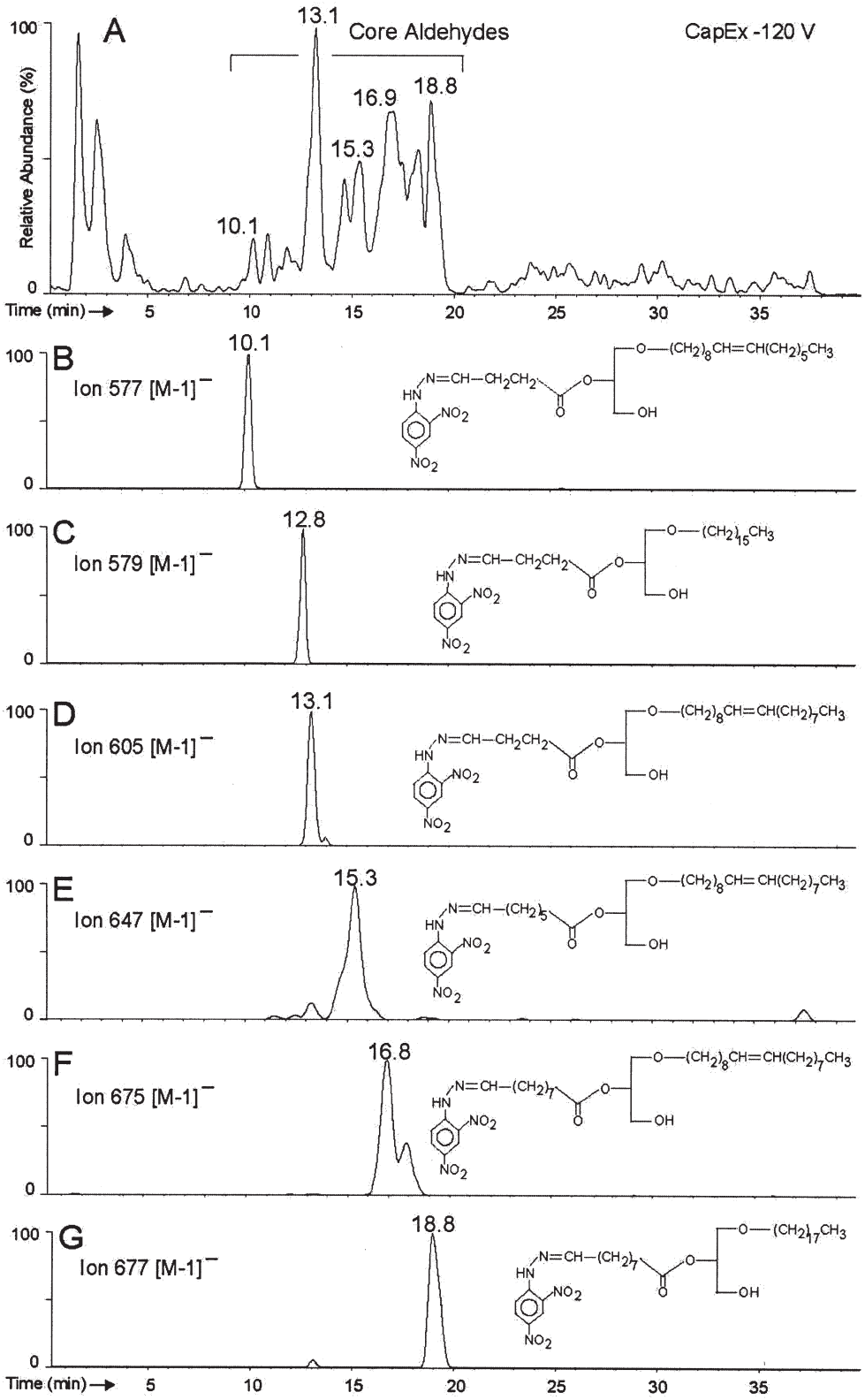

FIG. 4. Reversed-phase LC/ESI-MS analysis of autooxidized and DNPH derivatized 1-*O*-alkyl-2-oxoacyl-*sn*-glycerols from shark liver oil. (A) Total negative ion current profile of 1-*O*-alkyl-2-(DNPH-oxo)acyl-*sn*-glycerols. (B–G) reconstructed single-ion mass chromatograms of *m/z* 577, 579, 605, 647, 675, and 677 $[M - 1]^-$ diagnostic ions of 1-*O*-hexadecenyl-2-(DNPH-4-oxo)butyroyl-*sn*-glycerol, 1-*O*-hexadecyl-2-(DNPH-4-oxo)butyroyl-*sn*-glycerol, 1-*O*-octadecenyl-2-(DNPH-4-oxo)butyroyl-*sn*-glycerol, 1-*O*-octadecenyl-2-(DNPH-7-oxo)heptanoyl-*sn*-glycerol, 1-*O*-octadecenyl-2-(DNPH-9-oxo)nonanoyl-*sn*-glycerol, and 1-*O*-octadecyl-2-(DNPH-9-oxo)nonanoyl-*sn*-glycerol, respectively.

TABLE 4
Composition of Molecular Species of DNPH-Derivatized 1-*O*-Alkyl-2-Oxoacyl-sn-Glycerols Produced by Autooxidation of Pancreatic Lipase Treated Shark Liver Oil DAGE as Estimated by LC/ESI-MS[a]

Molecular species		1-*O*-Alkyl-2-DNPH-oxoacyl-*sn*-glycerol			
Carbon number	Tentative identification	ECN	RT (min)	$[M-1]^-$ (m/z)	Peak area
20:1 Ald	16:1-4:0 Ald	19	10.1	577	4.0
20:0 Ald	16:0-4:0 Ald	20	12.8	579	7.6
22:2 Ald	18:2-4:0 Ald	20	11.8	603	0.1
21:0 Ald	14:0-7:0 Ald 17:0-4:0 Ald	21	13.6	593	0.3
22:1 Ald	18:1-4:0 Ald (15:0-7:1 Ald)	21	13.1	605	21.9
22:0 Ald	18:0-4:0 Ald (15:0-7:0 Ald)	22	14.2	607	0.6
23:1 Ald	16:1-7:0 Ald 16:0-7:1 Ald	22	13.7	619	0.3
24:2 Ald	14:0-10:2 Ald 16:0-8:2 Ald 17:1-7:1 Ald	22	14.4	631	0.2
23:0 Ald	14:0-9:0 Ald 16:0-7:0 Ald †	23	15.1	621	2.2
24:1 Ald	17:1-7:0 Ald 20:1-4:0 Ald (17:0-7:1 Ald)†	23	14.6	633	4.7
25:2 Ald	18:1-7:1 Ald (14:0-11:2 Ald) (18:2-7:0 Ald)	23	15.0	645	2.2
25:1 Ald	18:1-7:0 Ald 16:1-9:0 Ald (18:0-7:1 Ald)	24	15.3	647	11.3
25:0 Ald	16:0-9:0 Ald (18:0-7:0 Ald)	25	16.6	649	2.4
26:1 Ald	16:0-10:1 Ald 17:1-9:0 Ald	25	16.5	661	1.7
27:2 Ald	17:1-10:1 Ald 20:1-7:1 Ald (14:0-13:2 Ald) (16:0-11:2 Ald) (18:2-9:0 Ald)	25	16.1	673	1.8
26:0 Ald	15:0-11:0 Ald 17:0-9:0 Ald 19:0-7:0 Ald	26	17.5	663	0.1
27:1 Ald	18:1-9:0 Ald (20:1-7:0 Ald)	26	16.9	675	18.7
28:2 Ald	18:1-10:1 Ald (16:1-12:1 Ald) (18:0-10:2 Ald)	26	17.4	687	6.9
27:0 Ald	18:0-9:0 Ald 16:0-11:0 Ald	27	18.8	677	6.9
28:1 Ald	16:0-12:1 Ald 18:0-10:1 Ald	27	17.4	689	0.4
29:2 Ald	16:0-13:2 Ald (19:0-10:2 Ald)	27	18.2	701	4.5
29:1 Ald	18:1-11:0 Ald 20:1-9:0 Ald (22:1-7:0 Ald)	28	18.9	703	1.3
30:2 Ald	18:1-12:1 Ald 20:1-10:1 Ald	28	19.0	715	0.1

[a]Average of two determinations. ECN, equivalent carbon number; RT, retention time; Peak area, percent of cumulative peak area of recovered $[M-1]^-$ ions; Ald, aldehyde.

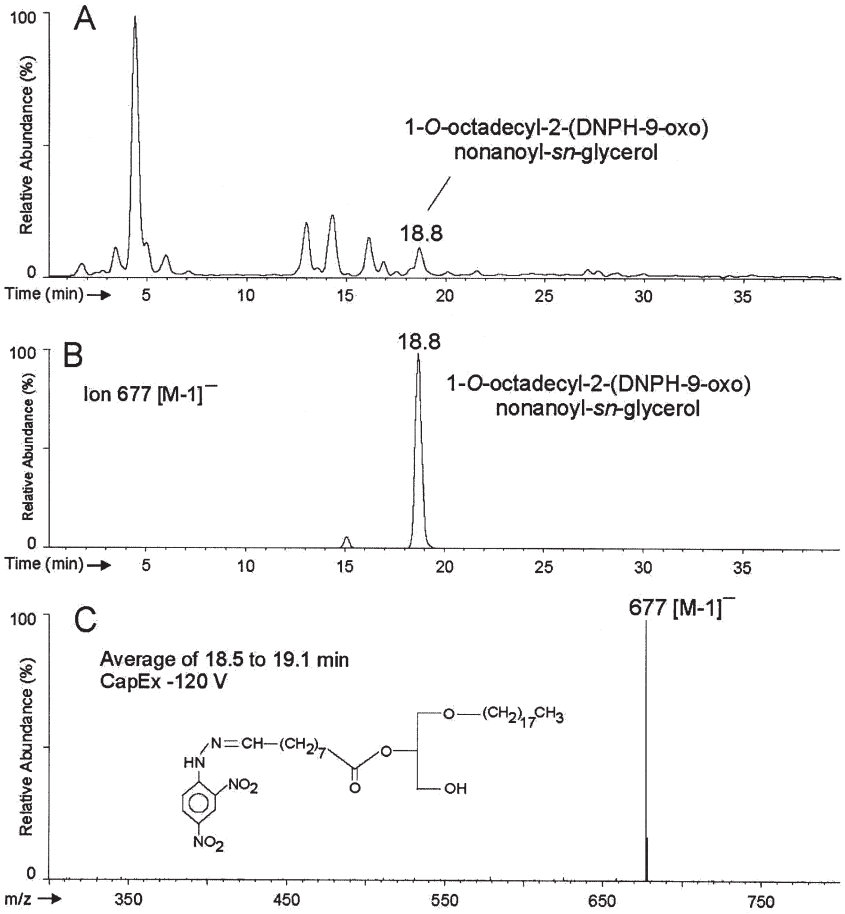

FIG. 5. Reversed-phase LC/ESI-MS analysis of autooxidized and DNPH derivatized 1-*O*-alkyl-2-acyl-*sn*-glycerols from human milk. (A) Total negative ion current profile. (B) Reconstructed single-ion chromatogram of the *m/z* 677 $[M - 1]^-$ diagnostic ion of 1-*O*-octadecyl-2-(DNPH-9-oxo)nonanoyl-*sn*-glycerol. (C) Full mass spectra averaged over the entire peak of 1-*O*-octadecyl-2-(DNPH-9-oxo)nonanoyl-*sn*-glycerol (zoomed to *m/z* 300–800) in (A).

Core aldehyde–containing triacylglycerols have been isolated from autoxidized vegetable oils (13,14) and from pig plasma lipoproteins following feeding of peroxidized fats and oils (15). Others have recovered core aldehyde–containing cholesteryl esters from autoxidized synthetic and natural (30) PUFA esters of cholesterol and from atheroma tissue (31). The present study describes the isolation and characterization of $C_{4:0}$ and $C_{5:0}$ core aldehydes from polyunsaturated diacylglycerol ethers from shark liver oil, and $C_{9:0}$ core aldehydes from human milk fat, which had not been previously reported.

Of special interest is the identification of the $C_{4:0}$ aldehyde (originating from 22:6n-3) ester in combination with the abundant 18:1n-9 alkyl moiety (50%), that is, 1-*O*-octadecenyl-2-(4-oxo)butyroyl-*sn*-glycerol, which, because of the shorter *sn*-2 chain length, could provide a higher affinity for the PAF receptor than the corresponding $C_{5:0}$ derivative, originating from 20:4n-6 esters. The 22:6n-3 (4.1% of *sn*-2 position) is highly susceptible to oxidation, and may, when esterified, yield a wide spectrum of short-chain core aldehydes with several double bonds by β-cleavage (32), such as $C_{4:0}$, $C_{7:1}$, $C_{8:2}$, and $C_{10:2}$. Another FA, highly susceptible to oxidation, is 22:5n-3 (1.6% of *sn*-2-position). This FA can yield the $C_{7:0}$ core aldehyde along with other core aldehydes with one or more double bonds. Oxidation of the remaining *sn*-2 FA would yield the $C_{9:0}$, $C_{11:0}$, $C_{12:1}$, and $C_{13:2}$ core aldehydes. We were able to characterize the *sn*-2 $C_{4:0}$, $C_{7:0}$, $C_{9:0}$, and $C_{10:1}$ short-chain aldehydes in combination with *sn*-1 18:1n-9-alkyl moiety as "free" core aldehydes.

Potential precursors of PAF mimics were also anticipated in human milk. However, we were able to identify only the 1-*O*-alkyl-2-(9-oxo)nonanoyl-*sn*-glycerol. The fatty alcohol and FA profiles of human milk preparation had previously been analyzed in our laboratory (17). The total composition was 16:0 (24%), 17:0 (2%), 18:0 (43%), and 18:1n-9 (31%) for the fatty alcohols and 16:1n-7 (3%), 18:1n-9 (36%), 18:2n-6 (5%), and 20:1n-9 (1%) for the unsaturated FA. Mild autooxidation would mainly affect the 18:2n-6 (29), and yield $C_{9:0}$ core aldehydes with minor quantities of $C_{12:1}$. Besides, oxidation of monounsaturates would yield the $C_{9:0}$ core aldehydes as well, with the exception of 20:1n-9 (1%). In other words, mild autooxida-

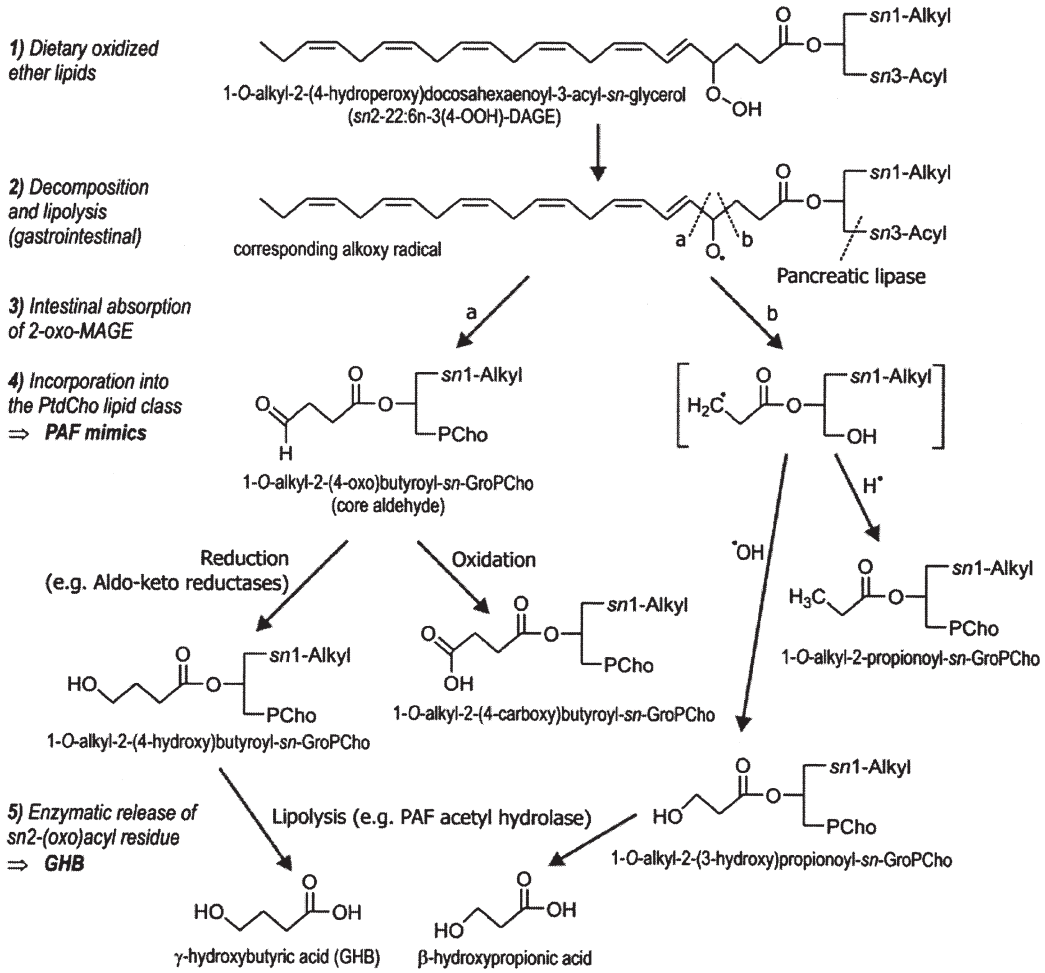

SCHEME 3. Proposed mechanism/pathway for formation of PAF mimics and GHB from DAGE containing docosahexaenoic acid.

tion of human milk would probably yield mainly the 1-*O*-octadecyl-2-(9-oxo)nonanoyl-*sn*-glycerol.

The isolation of the short-chain core aldehydes from the 1-*O*-alkyl-2-acyl-*sn*-glycerols is of special interest because it could lead to formation of mimics of PAF following intestinal absorption and entry into the CDP-choline pathway of PtdCho formation, bypassing the *de novo* step of diradylglycerol formation. A possible mechanism/pathway leading from a common DAGE to a PAF mimic is outlined in Scheme 3. Short-chain diacyl and diradylglycerols have been shown to be converted into short-chain PtdCho during incubation with appropriate enzymes and substrates (8). Because 1-*O*-alkylglycerols (28), and long-chain 2-*O*-alkylglycerols (28) are incorporated into glycerophospholipids following prior conversion into 1,2-diradyl-*sn*-glycerols in the intestinal microsomes, it is likely that the core aldehyde–containing 1,2-diradyl-*sn*-glycerols would also be incorporated into intestinal PtdCho to yield PAF mimics. According to Paltauf (28), the dietary 1-*O*-alkyl-*sn*-glycerols are preferentially incorporated into the glycerophosphoethanolamine *in vivo*, which, however, could be N-methylated to yield the corresponding GroPCho. Tanaka *et al.* (4) have discussed the PAF-like phospholipids formed during peroxidation of diacylglycerophosphocholines from different foodstuffs. A short-chain FA terminating in an aldehyde, hydroxyl, or carboxyl group located in the *sn*-2-position of 1-alkyl or 1-acyl glycerophosphocholine can mimic the action of natural PAF.

The short-chain core aldehydes of the *sn*-1-*O*-alkylglycerol would be expected to be readily absorbed by the intestinal mucosa because of their lower molecular weight, greater polarity, and overall similarity to monoacylglycerols. There is evidence for the intestinal uptake of intact short-chain diacylglycerols (6,7,33) as well as of oxygenated FA and acylglycerols (34–36). The presence of an alkyl group in the *sn*-1-position and a short-chain core aldehyde in the *sn*-2-position would render the molecule resistant to the endogenous lipases in the absence of isomerization, as already shown for pancreatic lipase.

The alkylglycerol core aldehydes would be expected to exhibit many of the metabolic properties of the core aldehydes of acylglycerols. Thus, these aldehydes would be expected to form Schiff bases, as demonstrated with the core aldehydes of 2-monoacylglycerols (16), and the core aldehydes of PtdCho (37) and cholesteryl esters (38). In fact, the adducts of the alkyl ether core aldehydes would be anticipated to be more resistant

to a detachment from the polypeptide and protein molecules because of the presence of the alkyl ether group. We have shown elsewhere (9) that the core aldehydes of alkyl glycerophosphocholines in atheroma induce platelet aggregation and inhibit endothelium-dependent arterial relaxation.

Furthermore, it is possible that the C_4 core aldehydes of alkylglycerols as well as of acylglycerols might be reduced by aldol-keto reductases to the corresponding C_4 core alcohols, which upon lipolysis would be released as GHB. The reduction of C_4 core aldehydes of glycerophosphocholine has already been demonstrated by Srivastava *et al.* (10), and the hydrolysis of C_4 core alcohol containing glycerophosphocholines to GHB has also been shown (4). Scheme 2 outlines a plausible mechanism/pathway for the formation of GHB from a DAGE containing a docosahexaenoic acid. Although the reduction of triacylglycerol core aldehydes to the corresponding core alcohols has not been specifically shown, such a reduction has been demonstrated for the neutral cholesteryl ester core aldehydes (Bhatnagar, 2006, personal communication). The broad substrate specificity of the aldol-keto reductases (39) promises that such reductions would take place also with triradylglycerol core aldehydes. The C_4 core alcohol groups associated with the primary positions of the triradylglycerol or triacylglycerol molecule would be anticipated to be readily released by the lingual and gastric lipases, which preferentially attack the short-chain FA (40). Any C_4 core alcohol groups associated with the secondary position of the glycerol molecule would have to undergo isomerization to a primary position before enzymatic release, as the *sn*-2-position is not known to be attacked directly.

In the brain, GHB is known to be formed from gamma-aminobutyric acid (GABA) (41) as well as from succinic semialdehyde (SSA) derived from GABA via a specific SSA reductase. The endogenous brain levels of GHB (2–5 nmol/g) are believed to be too low to stimulate $GABA_B$ receptors (K_i between 80 and 120 μM), although the synaptic cleft concentration is not known (42). Cortical GHB concentrations approaching 250 nmol/g, which are sufficient to stimulate $GABA_B$ receptors have been obtained by administration of 100–400 mg/kg of exogenous GHB (43). In any event, exogenously administered GHB causes a wide range of physiological and pharmacological properties, including addiction, tolerance, withdrawal, and intoxication, which are probably mediated via the $GABA_B$ receptor (44). This review shows that dietary sources are likely to contribute readily metabolizable precursors of GHB, the supply of which would increase with the increased consumption of omega-3 FA that is currently being actively promoted.

ACKNOWLEDGMENTS

The authors thank Dr. Robert C. Murphy, Department of Pharmacology, University of Colorado at Denver, for advice on interpretation of the mass spectra, and Dr. John J. Myher, Banting and Best Department of Medical Research, University of Toronto, for advice on ether lipid analysis. The crude deep-sea shark liver oil was a kind gift from Baldur Hjaltason, LYSI Ltd., Reykjavik, Iceland. This work was supported by funds from the Heart and Stroke Foundation of Ontario (Toronto, Ontario, Canada), the Medical Research Council of Canada (Ottawa, Ontario, Canada), the Association of Fish Meal and Fish Oil Manufacturers in Denmark (Copenhagen, Denmark), Danisco Ingredients (Aarhus, Denmark), and the Danish FØTEK Research Program.

REFERENCES

1. Whatley, R.E., Zimmerman, G.A., Prescott, S.M., and McIntyre, T.M. (1996) Platelet-Activating Factor and PAF-Like Mimetics, in *Handbook of Lipid Research,* vol. 8: *Lipid Secondary Messengers,* Bell, R.M., Exton, J.H., and Prescott, S.M., eds., pp. 239–276, Plenum Press, New York.
2. Mamelak, M., and Hyndman, D. (2002) Gammahydroxybutyrate and Oxidative Stress, in *Gammahydroxybutyrate: Molecular, Functional and Clinical Aspects,* Tunnicliff, G., and Cash, C.D., eds., pp. 218–235, Taylor & Francis, London.
3. Tokumura, A. (1995) A Family of Phospholipid Autacoids: Occurrence, Metabolism and Bioactions, *Prog. Lipid Res. 34*, 151–184.
4. Tanaka, T., Tokumura, A., and Tsukatani, H. (1995) Platelet-Activating Factor (PAF)-Like Phospholipids Formed During Peroxidation of Phosphatidylcholines from Different Foodstuffs, *Biosci. Biotech. Biochem. 59,* 1389–1393.
5. Kern, H., Volk, T., Knauer-Schiefer, S. , Mieth, T., Rüstow, B., Kox, W.J., and Schlame, M. (1998) Stimulation of Monocytes and Platelets by Short-Chain Phosphatidylcholines with and without Terminal Carboxyl Group, *Biochim. Biophys. Acta 1394,* 33–42.
6. Yang, L.Y., Kuksis, A., Myher, J.J., and Marai, L. (1992) Absorption of Short Chain Triacylglycerols from Butter and Coconut Oil, *INFORM 3,* 551. Abstract No III4.
7. Kuksis, A. (1986) Effect of Dietary Fat on Formation and Secretion of Chylomicrons and Other Lymph Lipoproteins, in *Fat Absorption,* vol. 2, Kuksis, A., ed., pp. 135–166, CRC Press, Boca Raton, FL.
8. Lehner, R., and Kuksis, A. (1992) Utilization of 2-Monoacylglycerols for Phosphatidylcholine Biosynthesis in the Intestine, *Biochim. Biophys. Acta 1125,* 171–179.
9. Kamido, H., Eguchi, H., Ikeda, H., Imaizumi, T., Yamana, K., Hartvigsen, K., Ravandi, A., and Kuksis, A. (2002) Core Aldehydes of Alkyl Glycerophosphocholines in Atheroma Induce Platelet Aggregation and Inhibit Endothelium-Dependent Arterial Relaxation, *J. Lipid Res. 43,* 158–166
10. Srivastava, S., Spite, M., Trent, J.O, Wes, M.B., Amed, Y., and Bhatnagar, A. (2004) Aldose Reductase–Catalyzed Reduction of Aldehyde Phospholipids, *J. Biol. Chem. 29,* 53395–53406.
11. Kuksis, A., Myher, J.J., Marai, L., and Geher, K. (1993) Hydroperoxides and Core Aldehydes of Triacylglycerols, in *Proceedings of 17th Nordic Lipid Symposium,* Malkki, Y., ed., Lipidforum, Bergen, Norway, pp. 230–238.
12. Byrdwell, W.C., and Neff, W.E. (1999) Non-volatile Products of Triolein Produced at Frying Temperatures Characterized Using Liquid Chromatography with Online Mass Spectrometric Detection, *J. Chromatogr. A 852*, 417–432.
13. Byrdwell, W.C., and Neff, W.E. (2002) Dual Parallel Electrospray Ionization and Atmospheric Pressure Chemical Ionization Mass Spectrometry (MS), MS/MS and MS/MS/MS for the Analysis of Triacylglycerols and Triacylglycerol Oxidation Products, *Rapid Commun. Mass Spectrom. 16*, 300–319.
14. Sjovall, O., Kuksis, A., and Kallio, H. (2003) Tentative Identification and Quantification of TAG Core Aldehydes as Dinitrophenylhydrazones in Autoxidized Sunflowerseed Oil Using Reversed Phase HPLC with Electrospray Ionization MS, *Lipids 38*, 1179–1190.

15. Suomela, J.-P., Ahotupa, M., and Kallio, H. (2005) Triacylglycerol Oxidation in Pig Lipoproteins After a Diet Rich in Oxidized Sunflower Seed Oil, *Lipids 40,* 437–444.
16. Kurvinen, J.-P., Kuksis, A., Ravandi, A., Sjövall, O., and Kallio, H. (1999) Rapid Complexing of Oxoacylglycerols with Amino Acids, Peptides and Aminophospholipids, *Lipids 34*, 299–305.
17. Kuksis, A., Marai, L., Myher, J.J., Cerbulis, J., and Farrell, H.M., Jr. (1986) Comparative Study of the Molecular Species of Chloropropanediol Diesters and Triacylglycerols in Milk Fat, *Lipids 21*, 183–190.
18. Myher, J.J., Kuksis, A., and Pind, S. (1989) Molecular Species of Glycerophospholipids and Sphingomyelins of Human Erythrocytes: Improved Method of Analysis, *Lipids 24,* 396–407.
19. Ravandi, A., Kuksis, A., Myher, J.J., and Marai, L. (1995) Determination of Lipid Ester Ozonides and Core Aldehydes by High-Performance Liquid Chromatography with On-line Mass Spectrometry, *J. Biochem. Biophys. Methods 30,* 271–285.
20. Kim, H.-Y., Wang, T.-CL., and Ma, Y.-C. (1994) Liquid Chromatography/Mass Spectrometry of Phospholipids Using Electrospray Ionization, *Anal. Chem. 66,* 3977–3982.
21. Myher, J.J., Kuksis, A., Tilden, C., and Oftedal, O.T. (1994) A Cross-Species Comparison of Neutral Lipid Composition of Milk Fat of Prosimian Primates, *Lipids 29*, 411–419.
22. Myher, J.J., Kuksis, A., and Yang, L.-Y. (1990) Stereospecific Analysis of Menhaden Oil Triacylglycerols and Resolution of Complex Polyunsaturated Diacylglycerols by Gas-Liquid Chromatography on Polar Capillary Columns, *Biochem. Cell Biol. 68*, 336–344.
23. Myher, J.J., Kuksis, A., Geher, K., Park, P.W., and Diersen-Schade, D.A. (1996) Stereospecific Analysis of Triacylglycerols Rich in Long-Chain Polyunsaturated Fatty Acids, *Lipids 31*, 207–215.
24. Esterbauer, H., and Cheeseman, K.H. (1990) Determination of Aldehydic Lipid Peroxidation Products: Malonaldehyde and 4-Hydroxynonenal, *Methods Enzymol. 186,* 407–421.
25. Ziegler, F.E., and Berger, G.D. (1979) A Mild Method for the Esterification of Fatty Acids, *Synth. Commun. 9*, 539–543.
26. Hartvigsen, K., Ravandi, A., Bukhave, K., Holmer, G., and Kuksis, A. (2001) Regiospecific Analysis of Neutral Ether Lipids by Liquid Chromatography/Electrospray Ionization/Single Quadrupole Mass Spectrometry: Validation with Synthetic Compounds, *J. Mass Spectrom. 36*, 1116–1124.
27. Itabe, H. (1998) Oxidized Phospholipids as a New Landmark in Atherosclerosis, *Prog. Lipid Res. 37*, 181–207.
28. Paltauf, F. (1971) Metabolism of the Enantiomeric 1-*O*-Alkyl Glycerol Ethers in the Rat Intestinal Mucosa *in vivo*; Incorporation into 1-*O*-Alkyl and 1-*O*-Alk-1'-enyl Glycerol Lipids, *Biochim. Biophys. Acta 239*, 38–46.
29. Sola, R., La Ville, A.E., Richard, J.L., Motta, C., Bargallo, M.T., Girona, J., Masana, L., and Jacotot, B. (1997) Oleic Acid Rich Diet Protects Against the Oxidative Modification of High Density Lipoprotein, *Free Radic. Biol. Med. 22*, 1037–1045.
30. Hoppe, G., Ravandi, A., Herrera, D., Kuksis, A., and Hoff, H.F. (1997) Oxidation Products of Cholesteryl Linoleate are Resistant to Hydrolysis in Macrophages, Form Complexes with Proteins and Are Present in Human Atherosclerotic Lesions, *J. Lipid Res. 38,* 1347–1360.
31. Ravandi, A., Babaei, S., Leung, R., Monge, J.C., Hoppe, G., Hoff, H., Kamido, H., and Kuksis, A. (2004) Phospholipids and Oxophospholipids in Atherosclerotic Plaques at Different Stages of Plaque Development, *Lipids 39,* 97–107.
32. Esterbauer, H., Zollner, H., and Schaur, R.J. (1991) Aldehydes Formed by Lipid Peroxidation: Mechanisms of Formation, Occurrence, and Determination, in *Membrane Lipid Oxidation*, vol. 1, Vigo-Pelfrey, C., ed., pp. 239–268, CRC Press, Boca Raton, FL.
33. Bezard, J., and Bugaut, M. (1986) Absorption of Glycerides Containing Short, Medium, and Long Chain Fatty Acids, in J. Bezard, M. Bugaut, in *Fat Absorption*, vol. 1, Kuksis, A., ed., pp. 119–158, CRC Press, Boca Raton, FL.
34. Staprans, I., Rapp, J.H., Pan, X.M., and Feingold, K. R. (1993) The Effect of Oxidized Lipids in the Diet on Serum Lipoprotein Peroxides in Control and Diabetic Rats, *J. Clin. Invest. 92*, 638–643.
35. Staprans, I., Rapp, J.H., Pan, X.M., Kim, K.Y., and Feingold, K.R. (1994) Oxidized Lipids in the Diet Are a Source of Oxidized Lipids in Chylomicrons of Human Serum, *Arterioscler. Thromb. 14,* 1900–1905.
36. Staprans, I., Rapp, J.H., Pan, X.M., and Feingold, K.R. (1996) Oxidized Lipids in the Diet Are Incorporated by the Liver into Very Low Density Lipoproteins in Rats, *J. Lipid Res. 37*, 420–430.
37. Ravandi, A., Kuksis, A., Shaikh, N., and Jackowski, G. (1997) Preparation of Schiff Base Adducts of Phosphatidylcholine Core Aldehydes and Aminophospholipids, Amino Acids, and Myoglobin, *Lipids 32,* 989–1001.
38. Kawai, Y., Saito, A., Shibata, N., Kobayashi, M., Yamada, S., Osawa, T., and Uchida, K. (2003) Covalent Binding of Oxidized Cholesteryl Esters to Protein, *J. Biol. Chem. 278*, 21040–21049.
39. Srivastava, S., Watowich, S.J., Petrash, J.M., Srivastava, S.K., and Bhatnagar, A. (1999) Structural and Kinetic Determinants of Aldehyde Reduction by Aldose Reductase, *Biochemistry 38,* 42–54.
40. Dupuis, L., Canaan, S., Riviere, M., Verger, R., and Wicker-Planquart, C. (2001) Preduodenal Lipases and Their Role in Lipid Digestion, in *Intestinal Lipid Metabolism,* Mansbach, C.M, II, Tso, P., and Kuksis, A., eds., pp. 19–35, Kluwer Academic/Plenum Publishers, New York.
41. Wong, G.T., Gibson, K.M., and Snead, O.C., III (2004) From the Street to the Brain: Neurobiology of the Recreational Drug γ-Hydroxybutyric Acid, *Trends Pharmacol. Sci. 25*, 29–34.
42. Bernasconi, R., Mathivet, P., Otten, U., Bettler, B., Bischoff, S., and Marescaux, C. (2002) Part of the Pharmacological Actions of γ-Hydroxybutyrate Are Mediated by $GABA_B$ Receptors, in *Gamma-Hydroxybutyrate,* Tunnicliff, G., and Cash, C.D., eds., pp. 28–63, Taylor & Francis, London.
43. Snead, O.C. (1991) The γ-Hydroxybutyrate Model of Absence of Seizures: Correlation of Regional Brain Levels of γ-Hydroxybutyric Acid and γ-Hydroxybutyrolactone with Spike Wave Discharges, *Neuropharmacology 30,* 161–167.
44. Maitre, M. (1997) The γ-Hydroxybutyrate Signaling System in Brain: Organization and Functional Implications, *Progr. Neurobiol. 51*, 337–361.

[Received March 1, 2006; accepted July 31, 2006]